

Practical US of the forefoot

Stefano Bianchi

Received: 3 February 2014 / Accepted: 9 February 2014 / Published online: 13 March 2014
© Società Italiana di Ultrasonologia in Medicina e Biologia (SIUMB) 2014

Abstract Disorders affecting the forefoot are common in the clinical practice. Accurate history and physical examination are the mainstays of diagnosis but imaging modalities are frequently obtained to confirm the clinical suspicion and plan appropriate treatment. In this article we will present the ultrasound (US) technique of examination of the forefoot followed by a brief description of the normal US anatomy and of US appearance of the most frequent forefoot disorders; rheumatoid arthritis, osteoarthritis, overuse arthropathy, Morton neuromas, bursitis, mucoid cysts, foreign bodies, bone disorders.

Keywords Forefoot · Ultrasound · Rheumatoid arthritis · Osteoarthritis · Overuse arthropathy · Morton neuromas · Bursitis · Mucoïd cysts · Foreign bodies

Riassunto Le patologie che interessano l'avampiede sono frequenti nella pratica clinica. L'anamnesi accurata e l'esame fisico sono i pilastri della diagnosi, ma le modalità di imaging sono spesso necessarie per confermare il sospetto clinico e pianificare un trattamento appropriato. In questo articolo presenteremo la tecnica dell'esame ecografico dell'avampiede, seguita da una breve descrizione dell'anatomia ecografica e delle caratteristiche delle lesioni più frequenti nell'avampiede: artrite reumatoide, osteoartrosi, artropatia da sovraccarico, neuroma di Morton, borsite, cisti mucoide, corpi estranei, lesioni ossee.

Introduction

Disorders affecting the forefoot are common in the clinical practice. Accurate history taking and well-performed physical examination are the mainstays of diagnosis but imaging modalities are frequently obtained to confirm the clinical suspicion and plan appropriate treatment.

Standard radiograph examination is always obtained as the first-line study [1]. Radiographs allow assessment of bones and joints as well as calcifications of the par-articular soft tissues. Standing X-rays are invaluable in obtaining evaluation of changes due to weight bearing. Computed tomography is rarely obtained in the evaluation of the forefoot due to excellent resolution of standard radiographs. Magnetic resonance imaging (MRI) has wonderful capabilities including high tissue contrast and multiplanarity. MRI is however not widely available in every country, is expensive, not well accepted by every patients and has definite relative and absolute contraindications.

The recent advances in ultrasound (US) technology, including developments of high-resolution, electronic broadband transducers and enhanced software capabilities, have lead to an improvement in the assessment the musculoskeletal system [2]. US is cheap, well tolerated by patients, has no contraindications and allows dynamic examination of joints, tendons and nerves of the foot [2–5]. In addition, US can accurately guide local injections or other interventional procedures [6–13]. It is now considered, together with plain films, to be the first-line technique for forefoot imaging [3, 5]. The main disadvantages of US are limited assessment of internal structures of the joints, bones and bone marrow.

In this article we will present the US technique of examination of the forefoot followed by a brief description

S. Bianchi (✉)
CIM SA, Cabinet d'Imagerie Médical, route de Malagnou 40A,
1208 Geneva, Switzerland
e-mail: stefanobianchi@bluewin.ch

of the normal US anatomy and of US appearance of the most frequent forefoot disorders.

US technique of examination and normal US anatomy

A basic history and local physical examination must be obtained in all patients to focalize the US examination. This approach shortens significantly the examination time. Localized tenderness while increasing the pressure through the transducer helps in focusing the US examination and permits more in depth assessment of the affected structures. As every musculoskeletal examination the US examination of the forefoot is always a “clinical-sonographic examination” [5]. A standard radiograph study, including the A-P and oblique views, must be also always obtained before starting the examination since it is more panoramic than US and allows simultaneous evaluation of the bones and joints [1].

Due to the superficial location of most structures of the forefoot the US examination is performed with high-frequency transducers [3, 5]. We routinely use a 17–5 MHz, 38 mm, linear electronic broad band and a “Joystick”, 23 mm, 15–7 MHz transducers. The former is first used because of its larger field of view and better color Doppler capabilities. The smaller transducer is useful in examining the intermetatarsal spaces and guiding local injections.

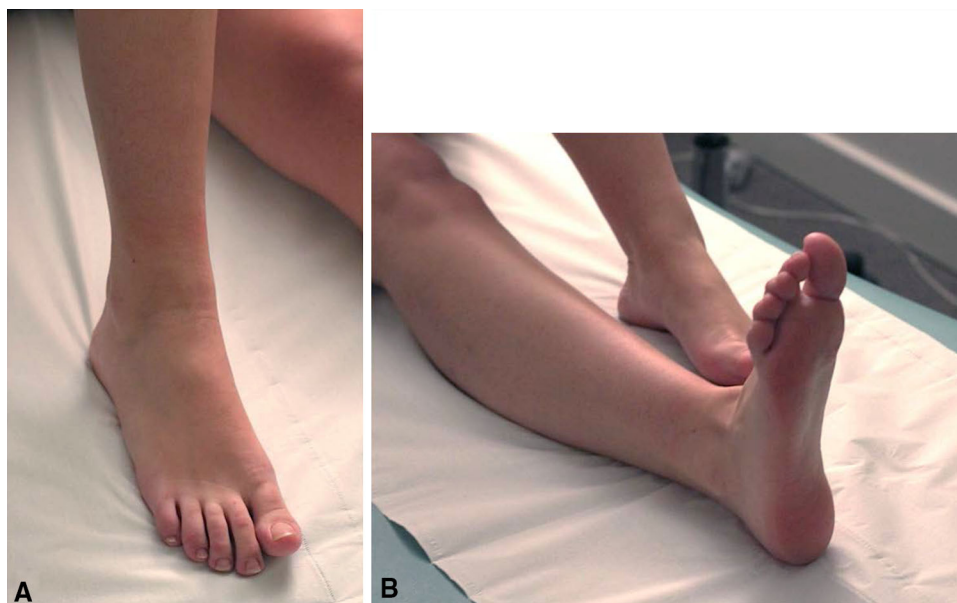
For routine US examination we use a two-position standard examination (Fig. 1).

Position 1

We start examining the patient supine with the knee flexed at 90° and the plant of the foot resting on the bed (Fig. 1a). This position allows adequate stabilization of the foot and ankle flexion resulting in extensor tendons stretching. We assess the dorsal aspect of the forefoot starting the examination at the level of the metatarsals and moving them distally over the metatarsophalangeal (MTP) and interphalangeal joints. Sagittal and transverse conventional and color Doppler sonograms are obtained over the skin and subcutaneous tissues, extensor tendons, metatarsals and forefoot joints as well as periarticular tissues [3, 5].

The extensor tendons appear as thin hyperechoic fibrillar bands running into the subcutaneous tissue. We first identify different tendons starting the examination at the anterior aspect of the ankle and then we follow them till the distal insertion trough transverse images. Longitudinal images are next obtained also during dynamic examination (flexo-extension of the toes). The cortical aspect of the metatarsals appears as a hyperechoic, continuous, regular line [14]. The normal periosteum is not detectable at US. The study of the intermetatarsal spaces by a dorsal approach is more difficult due to the difficulty to discriminate among the different structures. The MTP joints are well assessed by US. The synovial spaces located between the bone ends do not contain fluid in normal conditions. Only the first MTP joint can show a small fluid effusion in normal states. The normal synovial membrane is too thin to be detected. The cartilage of the metatarsal can be judged

Fig. 1 Technique of US examination position of the patient for scanning of the dorsal (a) and plantar (b) aspect of the forefoot



using dorsal and plantar sagittal images while the cartilage of the proximal phalanx is not appreciated. The interphalangeal joints are more difficult to be assessed because of their small size.

Position 2

Afterwards the patient is examined with the knee extended and the leg resting on the examination bed (Fig. 1b).

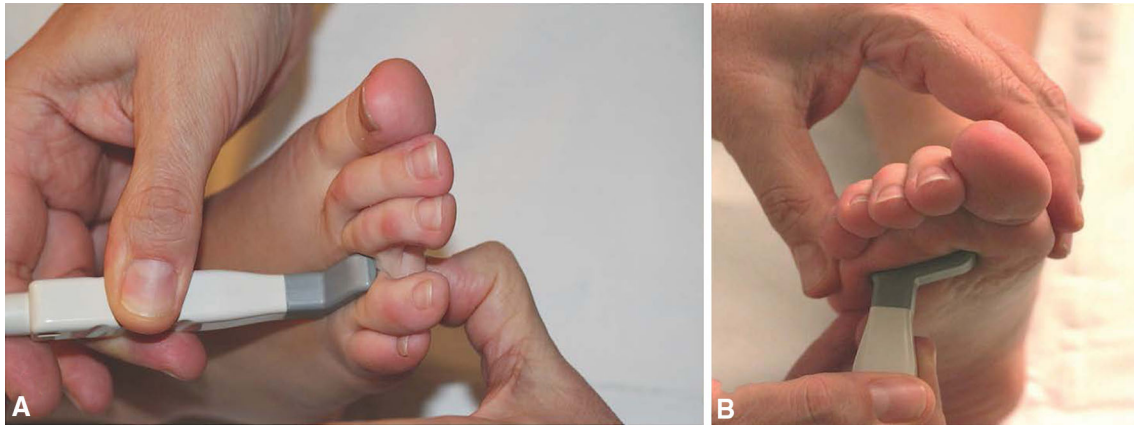


Fig. 2 Technique of US examination. Scanning technique for examination of the intermetatarsal spaces (a) and Mulder test (b)

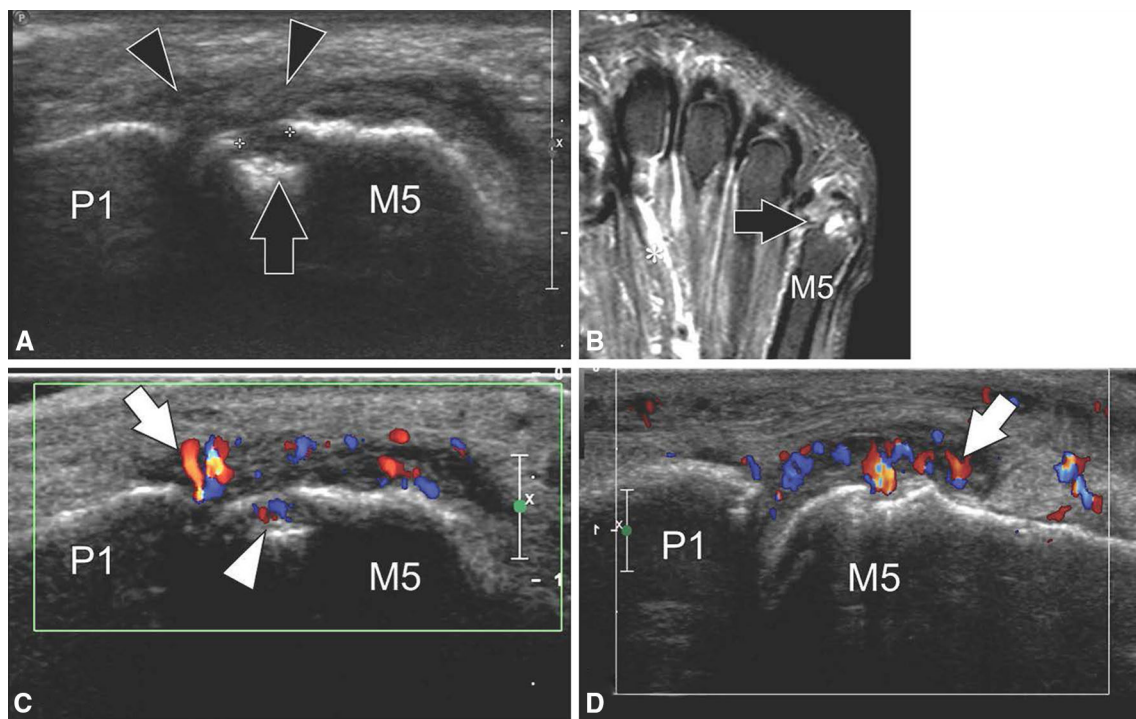


Fig. 3 Rheumatoid arthritis of the fifth MTP joint. **a** longitudinal sonogram obtained over the lateral aspect of the fifth MTP joint. **b** Corresponding T2-weighted MRI. **c, d** Color Doppler images obtained: **c** at the same level then (a); **d** at the dorsal aspect of the joint note marginal erosions (black arrows) on the lateral aspect of the

head of the metatarsal (M5) and hypoechoic synovial pannus (black arrowheads). Color Doppler shows hypervascular changes inside the pannus (white arrows) and the erosion (white arrowhead). P1 proximal phalanx

Transverse and sagittal images are obtained over the distal half of the plantar aspect of the foot. The skin, subcutaneous tissues and plantar fascia are examined followed by the flexor tendons and forefoot joints. Subsequently, without changing the patient's position, the intermetatarsal spaces are examined in sagittal and transverse plane using a dorsal approach while the examiner push with her/his non examining thumb on the plantar aspect of the space (Fig. 2a) [5]. Advantages of this method are basically three. First, the skin of the dorsal aspect is thinner and softer than that of the plantar aspect allowing better quality images. Second, local pressure trough the thumb widens the intermetatarsal space and decreases the thickening of the soft tissues resulting in their optimal judgement even when using high-resolution transducers. Finally, dynamic

examination performed applying different degree of thumb pressure and simultaneous anteroposterior movements permits better differentiation between a Morton neuroma (MN) and the frequently associated intermetatarsal bursitis. When performing the dynamic examination the patient is asked to report any local pain and to describe if this is the same occurring when walking. When the detection of MN is difficult (“thick” or “rigid” forefoots) we realize the so-called Mulder sonographic test. The test is performed by scanning on the plantar aspect of the forefoot during lateral compression of the metatarsal heads (Fig. 2b) [15]. If positive the examiner can see the MN displacing plantarly during compression. A “click” and a local pain are frequently associated to instability of the neuroma [5, 15].

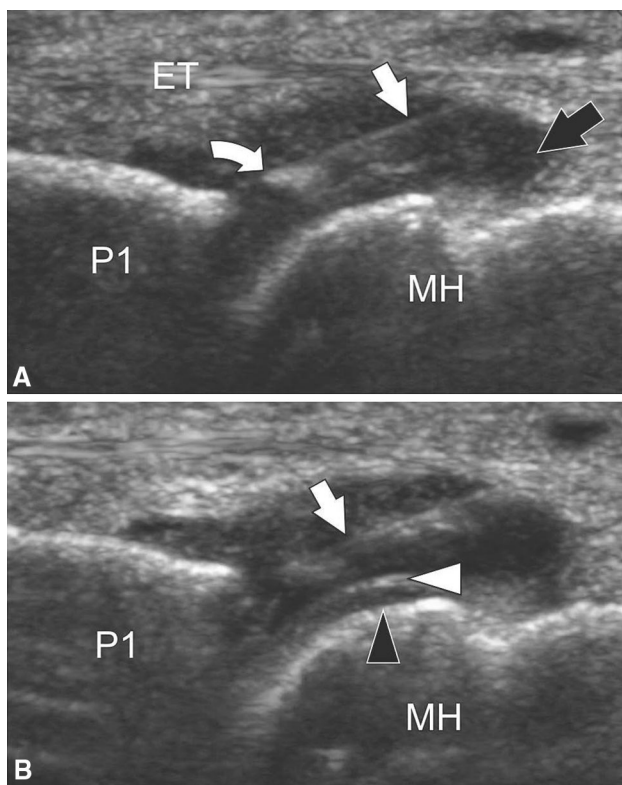


Fig. 4 US-guided joint injection in rheumatoid arthritis. **a, b** Longitudinal sonograms obtained over the dorsal aspect of the second MTP joint. In **a**, the joint cavity is filled by hypoechoic pannus (black arrow). The needle (white arrow), introduced inside the joint under US guidance, is easily depicted as a hyperechoic linear structure, its tip (curved arrow) can be clearly detected. In **b**, obtained after intraarticular injection of a few drops of steroids, note appearance of a hyperechoic interface (white arrowhead) over the cartilage (black arrowhead) confirming presence of intraarticular fluid P1 proximal phalanx, MH metatarsal head

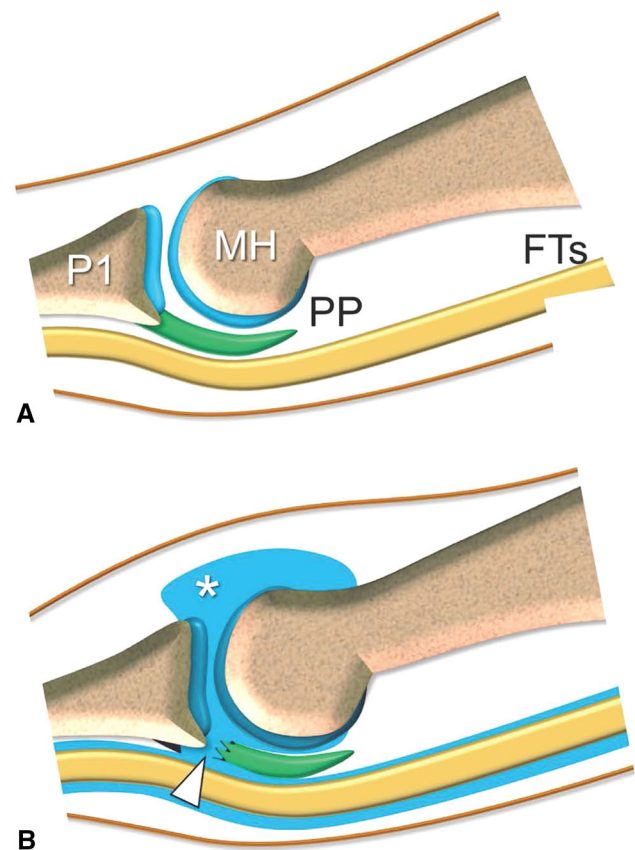


Fig. 5 Overuse of the MTP joints. Schematic sagittal drawings showing **a** the normal MTP joint and **b** changes due to chronic overuse. In **a** note the metatarsal head (MH), proximal phalanx (P1), joint plantar plate (PP) and the flexor tendons (FTs). In **b** due to chronic load at the plantar aspect of the joint a synovial effusion is seen inside the joint (asterisk) as well as in the flexor tendons sheath. The two effusions communicate trough a full-thickness tear of the plantar plate that appears avulsed from the proximal phalanx

US examination of the plantar aspect of the metatarsal region is difficult because of its complex anatomy. The elevator technique (repetitive axial scanning from proximal to distal and vice versa) is extremely useful to “follow” each structure in order to appreciate its size, echogenicity and relations with adjacent structures. Power Doppler makes easy the assessment of vessels. US examination of the plantar aspect of the MTP joints is performed by both axial and sagittal images. Sagittal images work best to study dynamically the plantar plates that appear as a hyperechoic bands inserting into the base of proximal phalanx [16, 17]. The normal plates present a maximal thickness at the distal insertion. Their proximal insertion cannot be assessed by US. Dynamic examination obtained during dorsal flexion of the examined toe is important in confirming full-thickness tears. In this case, the plate shows limited movements during extension of the toe. The flexor tendons can be followed by US till their distal insertion into the distal phalanx.

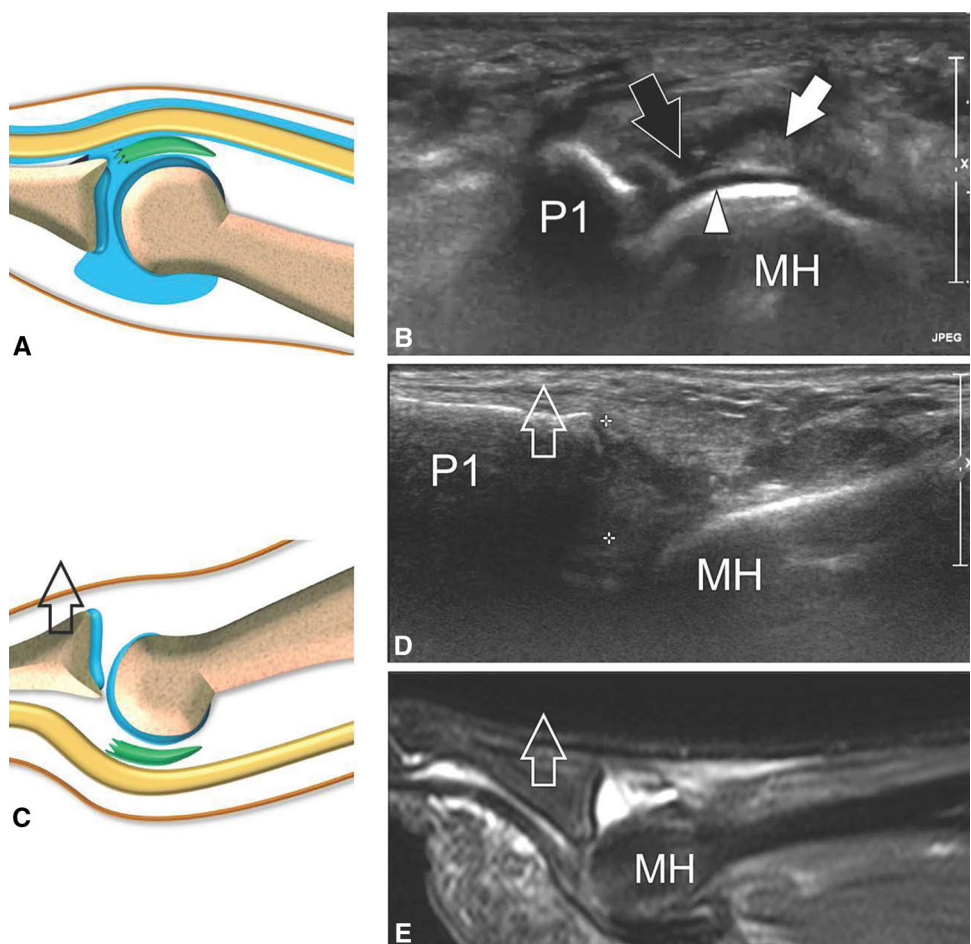
Pathologic changes

Joint disorders

Rheumatoid arthritis

In rheumatoid arthritis, hypertrophy of the synovial membrane (pannus) can fill partially or completely the joint space and lead to weakening of the capsuloligamentous structures, cartilage destruction, joint marginal erosions and marked functional impairment. US shows easily the rheumatoid pannus as a hypoechoic thickening of the synovial membrane with or without internal hypervascular signals at color Doppler, depending on disease activity (Fig. 3) [18]. Local erosions are imaged as focal interruption of the hypoechoic cartilage and hyperechoic subchondral bone. US is more sensitive than radiographs in detecting early erosive changes and allow an early diagnosis and aggressive treatment in order to decrease permanent joint damage. During examination attention must

Fig. 6 Overuse of the MTP joints. US appearance. **a**, **b** Schematic sagittal drawing (a) and corresponding sonogram (b) obtained over the plantar aspect of the joint. Note full-thickness tear (black arrow) of the plantar plate (white arrow) that is posteriorly retracted. Arrowhead joint cartilage (c–e). Schematic sagittal drawing (c), corresponding sonogram (d) and T2-weighted MR image (e) obtained over the dorsal aspect of the joint. Images show dorsal dislocation (void arrows) of the proximal phalanx (P1) with respect of the metatarsal head (MH)



be given to careful assessment of the MTP joints of the fifth toes and possible erosions of the fifth metatarsal heads due to early involvement of this joint in RA [19].

Intraarticular steroid injections of the MTP joints can be easily guided by US (Fig. 4) [8, 9, 13]. After careful local disinfection and generous use of skin disinfectant we examine the joint with a dorsal sagittal approach (patient

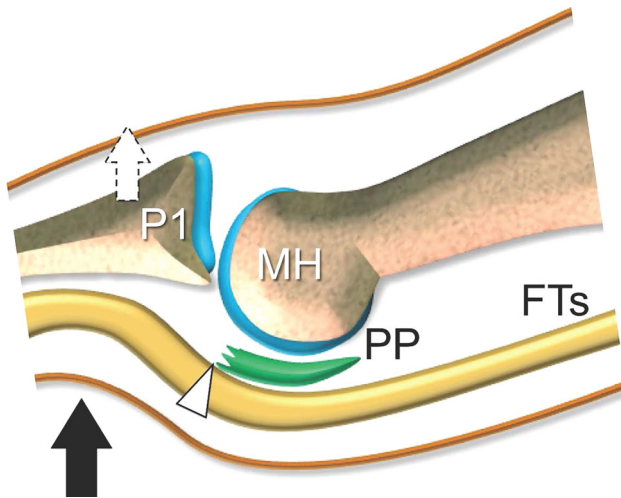
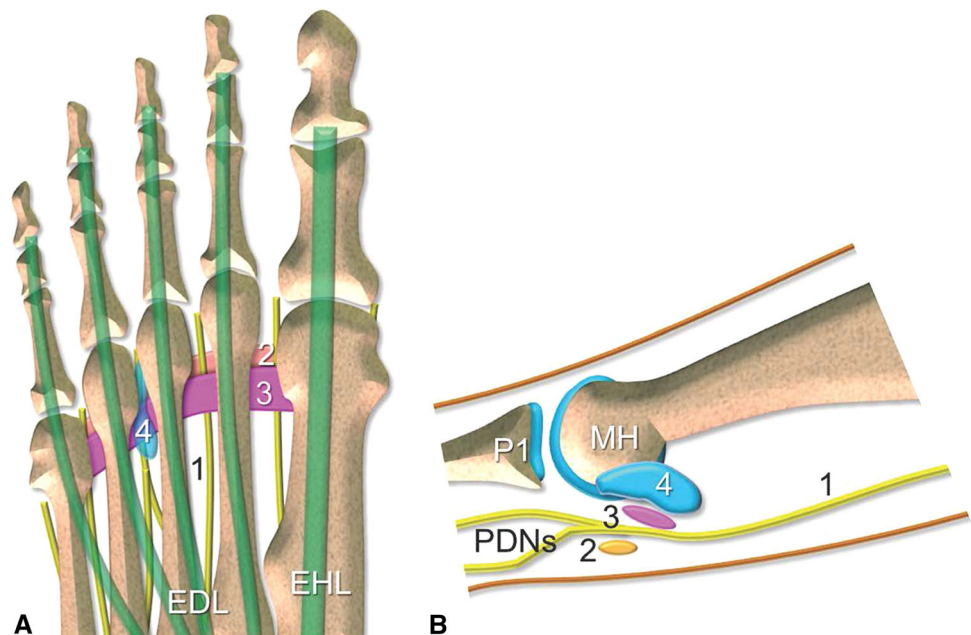


Fig. 7 Overuse of the MTP joints. Dynamic US. Sagittal drawing showing dorsal instability (dotted arrow) of the proximal phalanx (P1) due to full-thickness tear (arrowhead) of the plantar plate (PP). Black arrow non dominant thumb of the examiner displacing the patient's toe dorsally

Fig. 8 Anatomy of the digital nerves joints. Axial (a) and sagittal (b) drawings of the forefoot 1 common plantar digital nerve, PDNs proper digital nerve, 2 superficial intermetatarsal ligament, 3 deep intermetatarsal ligament, 4 intermetatarsal synovial bursa, P1 proximal phalanx, MH metatarsal head, EDL extensor digitorum longus tendon, EHL extensor hallucis longus tendon



position 1). The needle is inserted just proximal to the transducer, at the level of the distal metatarsal head, and advanced from posterior to anterior using an angle with the skin surface of approximately 45°. As the needle tip is identified the needle is followed by real-time US till its tip lies inside the joint space. Use of a 27 gauge/2–3 cm needle is almost painless and makes subcutaneous anesthesia unnecessary. The amount injected into the MTP joints is 0.3 cc of steroid mixed with 0.2–0.5 cc of lidocaine 1 %.

Tenosynovitis can also be associated to arthritis and appear as thickening of the synovial tendon sheath with or without associated fluid. The tendon structure can appear hypoechoic due to action of the pannus. Partial tears can be detected as thinning of the tendon. Complete tears are associated to tendon retraction. In difficult cases, dynamic examination can facilitate the differential diagnosis between partial and complete tears.

Osteoarthritis

Degenerative articular changes of the forefoot joints are mainly seen at the level of the first MTP joint (Hallux rigidus). Pathologic changes are well depicted by standard radiographs and US is not needed for the diagnosis. US shows the marginal osteophytosis as osseous beaks more evident at the dorsal aspect of the metatarsal head. Intra-articular effusion and mild hypertrophy of the synovium can be associated. Local hyperaemia is rare.

Overuse arthropathy

Overuse of forefoot joints is mainly seen at the MTP of the second toe due to chronic stress related to hallux valgus deformity (Fig. 5) [20]. A synovial intraarticular effusion is first seen followed by pathologic changes of the plantar plate. Focal partial tears of the plate are usually observed at its distal attachment and present as ill-defined hypoechoic irregular area [17, 21]. In larger full-thickness tears, proximal retraction of the plate is seen together with a joint effusion that can communicate with the flexor tendons' synovial sheath and appears as a hypoechoic halo surrounding the tendons (Fig. 6). In case of significant plate retraction, the flexor tendons can be seen resting on the plantar cartilage of the metatarsal head. Dynamic

examination during selective flexion/extension of the IP joints of the affected toe helps in detecting the position of the tendons. Dorsal flexion of the proximal phalanx is invaluable in confirming a large full-thickness tear by showing increase of the gap between the retracted plate and the base of the phalanx. US examination by a dorsal sagittal approach is best suited to judge dorsal instability of the proximal phalanx with respect of the metatarsal head. The distance between the two can be easily measured. Dynamic examination during concomitant upward pushing on the toe by the non examining hand is helpful in doubtful cases (Fig. 7).

Periarticular masses

Morton neuromas

Morton neuromas are the most frequent masses of the forefoot. They are fusiform thickening of the common

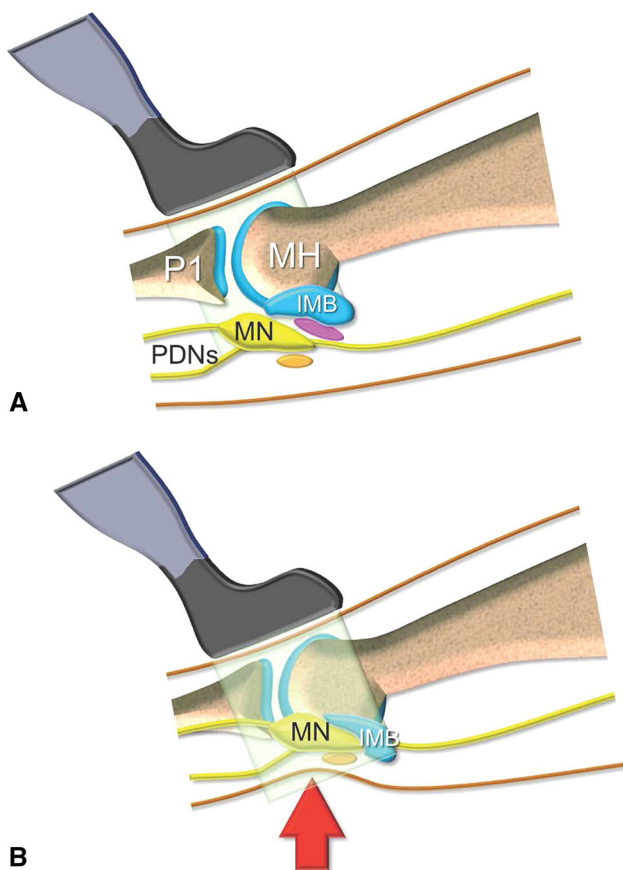
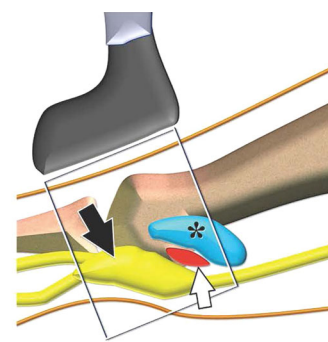


Fig. 9 US examination of Morton neuromas. Sagittal drawings showing dorsal scanning of a intermetatarsal space without (a) and with (b) application of plantar pressure through non dominant thumb of the examiner. In a the thickness of the soft tissue do not allow an optimal visualization of the Morton neuroma. In b the decrease of the soft tissue together with dorsal displacement of the neuroma allow its optimal assessment. MN Morton's neuroma, IMB intermetatarsal bursitis



A



B

Fig. 10 US appearance of Morton neuroma. Sagittal drawing (a) and corresponding sagittal sonogram (b) show a Morton neuroma (black arrows) associated with a fluid filled intermetatarsal bursitis (asterisk). Arrowheads common digital nerve, white arrows deep intermetatarsal ligament

interdigital nerves due to endo/perineural fibrosis related to chronic compression at the level of the anterior part of the intermetatarsal spaces [22]. At this level, the common plantar digital nerves run inferiorly to the deep intermetatarsal ligament and superficially to the deep intermetatarsal ligament (Fig. 8), to split then in the two proper digital nerves. The intermetatarsal synovial bursa lies between the metatarsal heads dorsally to the deep intermetatarsal ligament. The third metatarsal interdigital nerve is most frequently involved probably because its fixed position with respect to others nerves. Chronic trauma and frictions due to overload facilitated by incongruent shoes (high heels) lead to a degenerative reaction, fusiform thickening and internal fibrosis of the nerve. Repeated marked dorsiflexion of the toes is probably contributory of interdigital nerve entrapment. The patient report local excruciating pain and numbness and paraesthesia in the forefoot irradiating to the adjacent toes.

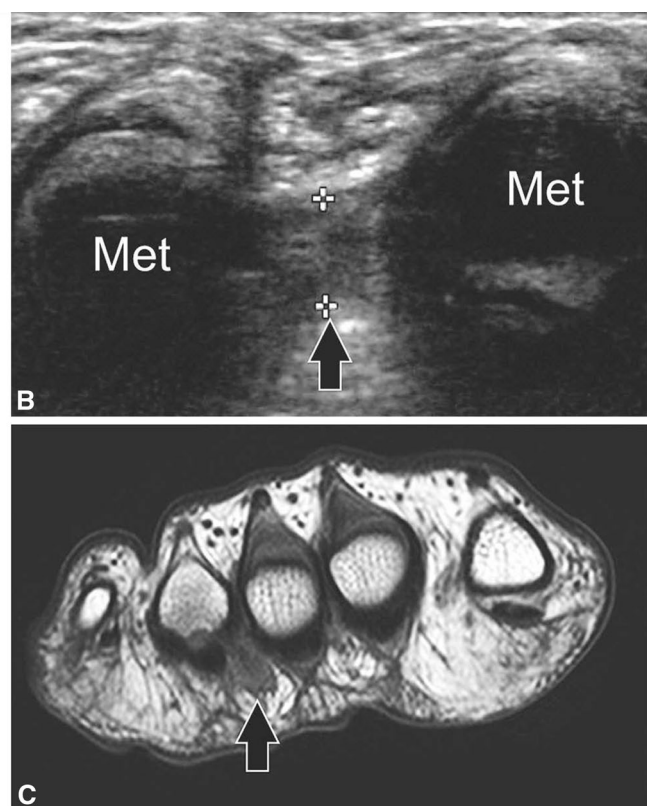
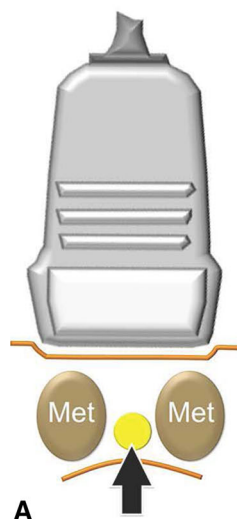
Ultrasound can detect Morton's neuroma and confirm the clinical diagnosis [23, 24]. US has demonstrated a high sensitivity and specificity in the diagnosis of plantar neuroma, and can help to provide their exact localization and size thus guiding surgery to the appropriate intermetatarsal space. As formerly reported, we prefer to examine the supine patient by a dorsal approach while applying a forceful pressure with the left thumb on the plantar aspect of the involved intermetatarsal space (Fig. 9). Dorsal

scanning is preferred to plantar examination because the thickness of the stratum corneum of the sole of the foot can limit propagation of the US beam. Pressure with the left thumb widens the intermetatarsal space and facilitates its assessment. We prefer to use longitudinal scans since they allow more evident demonstration of continuity of the hypoechoic neuroma with the interdigital nerve.

A MN appears at US as fusiform, well-delimited hypoechoic mass in continuity with the common digital nerve (Figs. 10, 11) [23, 24]. Use of high-frequency transducer allows frequently detection of the nerve also in normal conditions. US can also detect inflammatory changes of the intermetatarsal bursa such as thickening of the synovial wall and associated effusion. Dynamic examination obtained with application of different degree of pressure with the thumb facilitates differentiation between the neuroma and bursitis (Fig. 12).

Ultrasound is invaluable in guiding local injections in the treatment of MN [10–13, 25]. We use a dorsal approach and a 27G/3 cm needle (Fig. 13). After proper skin preparation the intermetatarsal space is scanned in the sagittal plane as shown in Fig. 13. Under real-time guidance the needle is introduced proximal to the clubfoot transducer at 45° and slowly advanced till its point is located inside the bursa. When an appropriate technique is used, no local anesthesia is needed because of the small needle size [26]. The procedure is almost always painless. We usually inject

Fig. 11 US appearance of Morton neuroma. Coronal drawing (a) and corresponding sagittal sonogram (b) and T1-weighted MRI image (c) show a Morton neuroma (black arrows). Plantar displacement of the neuroma in c is due to MRI examination in prone position. *Met* metatarsals



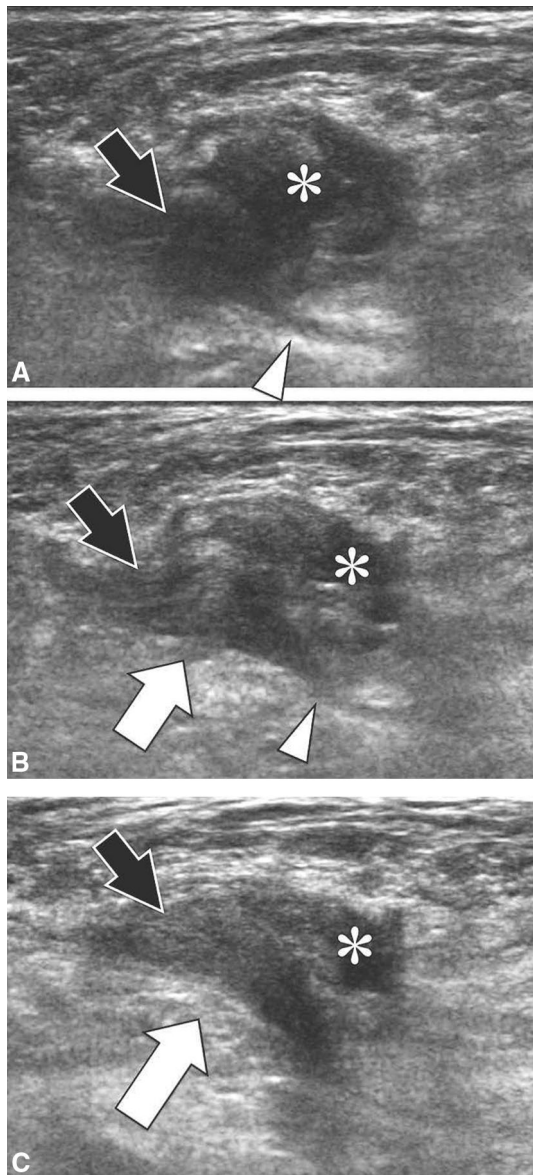


Fig. 12 US appearance of Morton neuroma. Dynamic examination. Sagittal sonograms obtained without (**a**) and with application of increasing pressure with the examiner's thumb (**b**, **c**). In **a** differentiation between the neuroma (*arrow*) and the bursitis (*asterisk*) is difficult. With application of increasing local pressure (*white arrows*) the bursa is displaced posteriorly and the neuroma dorsally allowing better differentiation between the two structures. *Arrowheads* common digital nerve

1 ml of a mixture of rapid and slowly acting steroid inside the bursa and around the neuroma. Progressive filling of the bursa can be followed during real-time examination. We entirely perform the procedure without any help from an assistant. We hold indifferently the transducer with the right or left hand and the syringe with the other hand. After a short learning curve (realization of 10/20 procedures), the entire procedure can be performed in nearly 1–2 min. The

patient is asked to assume analgesic in case of steroid flashes and avoid excessive walking for 3–4 days.

Bursitis

Depending on their location, synovial bursae of the fore-foot can be of two types: intermetatarsal and submetatarsal bursae. The latter are located in the subcutaneous tissues at the level of the metatarsal heads and are due to chronic local overload. Intermetatarsal bursitis can be concomitant to MN or found in arthritis (Fig. 14). Both types of bursitis are easily appreciated by US [27, 28]. Although they can contain some fluid most bursitis appear as hypoechoic masses due thickening of the synovial wall. Color Doppler can show internal hyperaemia. Dynamic examination is very important in their assessment since it helps in differentiating an inflamed bursa, that changes its shape and size, from an uncompressible solid mass. In addition, local pressure allows a more evident differentiation between the synovium and an internal effusion.

Muroid cysts

Muroid cysts are periarticular cystic lesions, filled by gelatinous fluid, presenting a fibrous wall that can communicate with the joint cavity or tendon sheath [29]. Depending on their location they can be painful because of compression of adjacent structures (nerves etc.). If located at the plantar aspect of the forefoot they can be painful during walk.

Ultrasound depicts muroid cysts as well-delimited hypoechoic masses adjacent to joints (Fig. 15). They can contain septa and show hypervascular changes of the wall when inflamed. US can help in guiding aspiration of the cyst and an internal injection.

Other masses

Pigmented villonodular synovitis is a benign proliferative disease of the synovium that can present in a diffuse form, affecting mainly the talocrural joint in the ankle and foot region, or as a nodular form also known as giant cell tumor of the tendons sheath [29–31]. The nodular form affects mainly the toes and presents at US as a homogeneous, hypoechoic, well-delimited solid mass in close contact with a tendon. Color Doppler can show some internal flow signals [31]. US assesses the relation of the mass with the adjacent tendons, vessels and nerves, detects bone pressure erosions and is helpful in detecting early local recurrence after surgical excision. The US appearance is aspecific and a definite diagnosis relies in MRI that shows a hypointense mass in T2-weighted images.

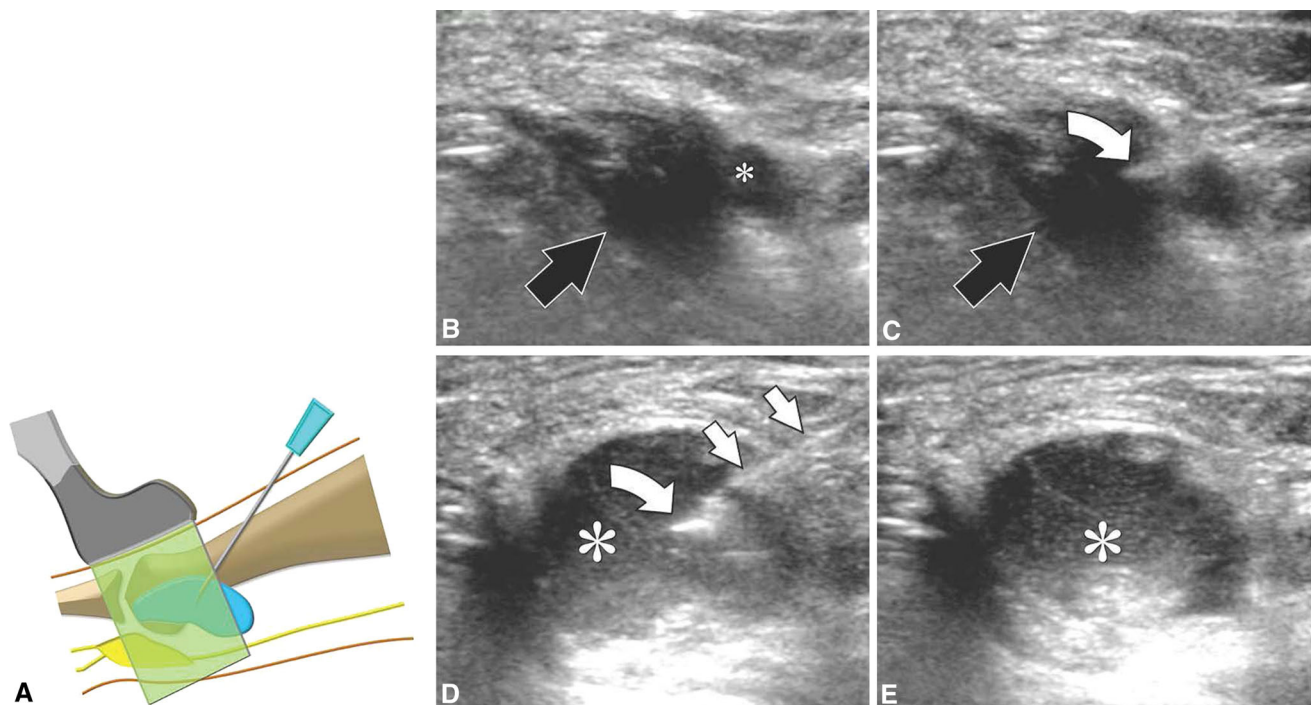


Fig. 13 US-guided injection of Morton neuroma. Sagittal drawing (a), corresponding sagittal sonograms (b–e) obtained during progressive injection of the intermetatarsal bursitis (b–d) and after needle

removal (e). *Black arrow* Morton neuroma, *small asterisk* intermetatarsal bursitis, *curved arrow* needle tip, *white arrows* needle, *large asterisks* injected steroid

Schwannoma and neurofibroma are benign tumors of the peripheral nerves appearing at US as hypoechoic well-margined masses that can be found along the course of a peripheral nerve [32, 33]. Demonstration of relationship of the mass with a nerve, when detectable at US, increases the diagnostic value. Vascular changes inside the tumors are variable, schwannoma being usually more vascularized than neurofibroma (Fig. 16).

Other masses such as fibroma, chondroma or malignant tumors can affect the forefoot, but are infrequent [34].

Foreign bodies

Forefoot foreign bodies (FBs) appear at US as hypoechoic structures with posterior artifact almost always found at the plantar aspect of the foot (Fig. 17) [2, 5, 35, 36]. A history of penetrating injury can be obtained, but not always. They can cause pain and, if unrecognized, lead to local infection. US can detect FBs, assess the distance from the skin and their size. Depending on the associated artifact, the nature of the fragment can be suspected. Metallic or glass fragments present a “comet tail” artifact, while bone or vegetable fragments are associated with posterior shadowing. The relation of FB with the adjacent anatomic (nerves, vessels, tendons, joints) structures can be easily judged. Assessment of the depth and exact location of the FB are necessary for

a successful surgical removal. Marking the skin with permanent ink or localising the FB by a needle [36] before surgical removal works well in facilitating fragment removal. US-guided removal has been proposed as a safe and less invasive option to surgical removal.

Bone disorders

Stress fractures can be divided into fatigue or insufficiency fractures. Fatigue fractures result from abnormal repetitive load on a normal bone as it can occur in military recruits or athletes. Insufficiency fractures follow normal stress on pathologic weak bones [37]. They frequently affect the metatarsals that are exposed to repetitive charges during prolonged walking. Patients report mechanical pain with exacerbation during weight-bearing activities.

Conventional radiographs are normal at first and show periosteal thickening only after several weeks. Although US has intrinsic limitations in the evaluation of bones it allows a good assessment of the dorsal surfaces of the metatarsals. US has been proved to be able to diagnose early stress fractures of the metatarsal bones when conventional radiographs are still normal [38, 39]. The US appearance includes focal thickening of the periosteum that shows hypervascular changes at color Doppler and rarely a focal interruption of the hyperechoic bone cortex

Fig. 14 US appearance of intermetatarsal bursitis in rheumatoid arthritis. Coronal sonogram (a) and corresponding coronal T1-weighted post Gd MR image (b). US shows thickening of the synovial wall (white arrow) of the bursa filled by fluid (black arrow) associated with an internal fluid neuroma (black arrows) associated with a intermetatarsal bursitis (asterisk). In b note contrast enhancement of the inflamed wall (arrowheads) and internal fluid. ET extensor tendons, MH metatarsal head

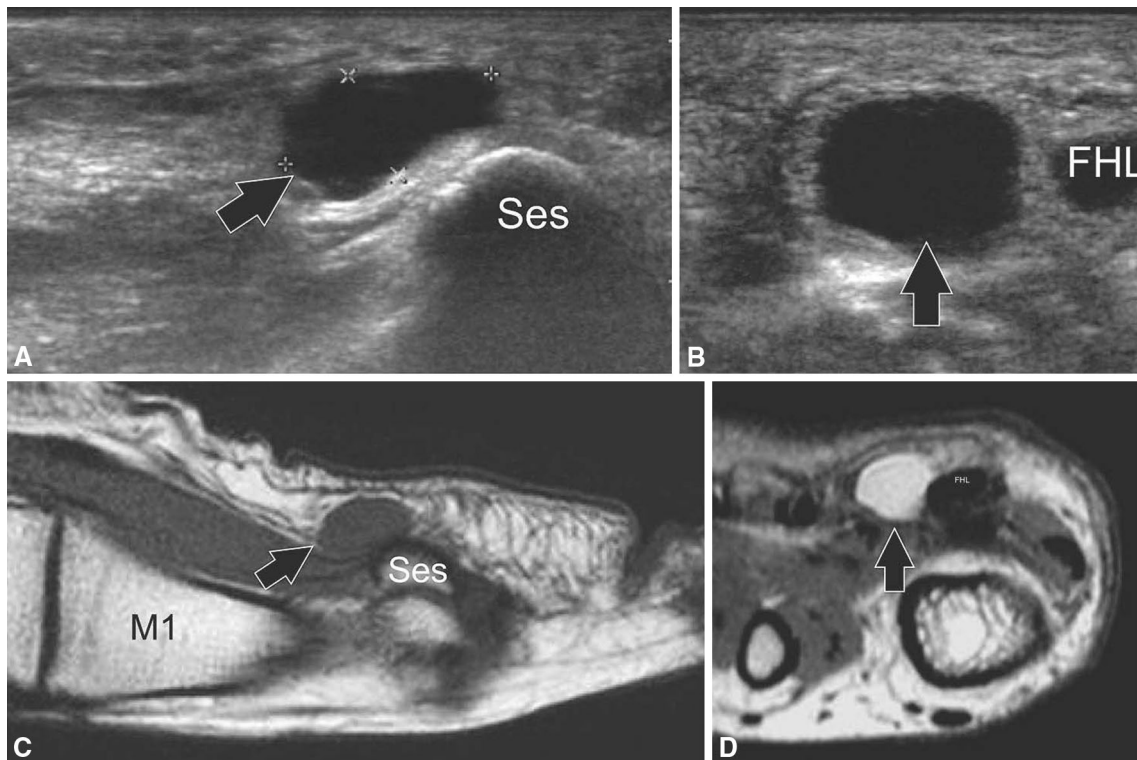
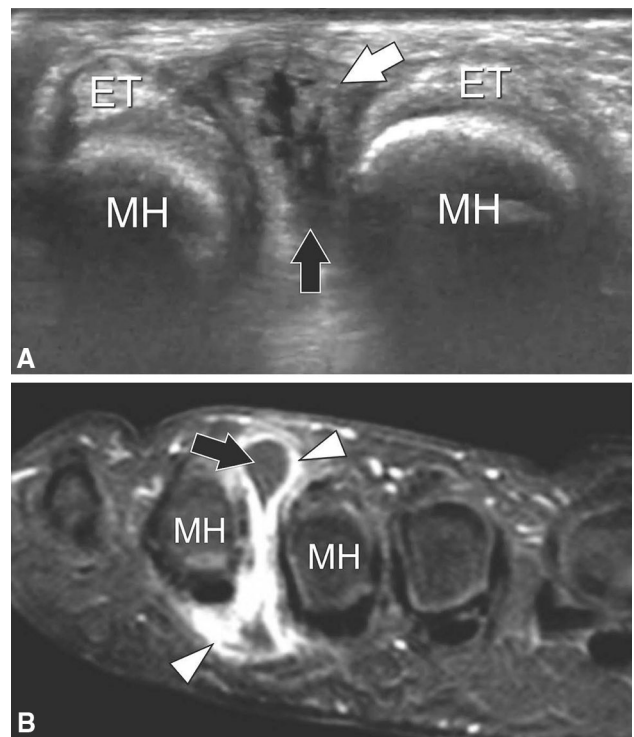


Fig. 15 US appearance of mucoid cyst. Sagittal (a) and coronal (b) sonogram and corresponding sagittal T1-weighted (c) and coronal T1-weighted (d) MR images US depicts the cyst (arrows) as an

anechoic fluid filled structure with sharp borders adjacent to the fibular sesamoid of the thumb (Ses) and the flexor hallucis longus tendon (FHL). MRI confirms the US findings

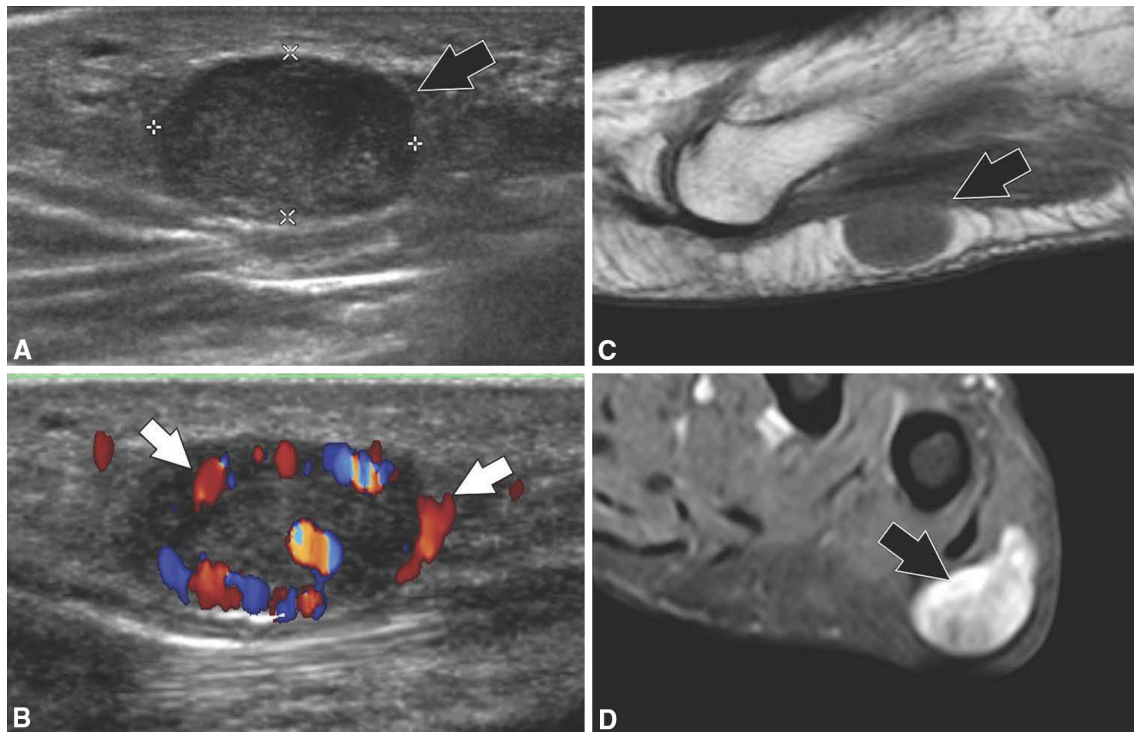


Fig. 16 US appearance of schwannoma. Sagittal (a) and sagittal color Doppler (b) sonogram and sagittal T1-weighted (c) and coronal T1-weighted post Gd (d) MR images US depicts the schwannoma (arrows) as an hypoechoic solid structure with sharp borders located

in the subcutaneous plantar tissues. In (b) note internal vascularisation. MRI shows a mass isointense in the T1-weighted sequence with irregular internal enhancement after Gadolinium injection

Fig. 17 US appearance of foreign body. Coronal (a) and coronal color Doppler (b) sonogram obtained at the level of the proximal phalanx (P1) of the second toe US depicts a wooden splinter (arrows) as an hypoechoic linear structure located into the soft tissues plantar to the phalanx. In b hypervascular signals into the adjacent soft tissues are consistent with a local inflammatory reaction

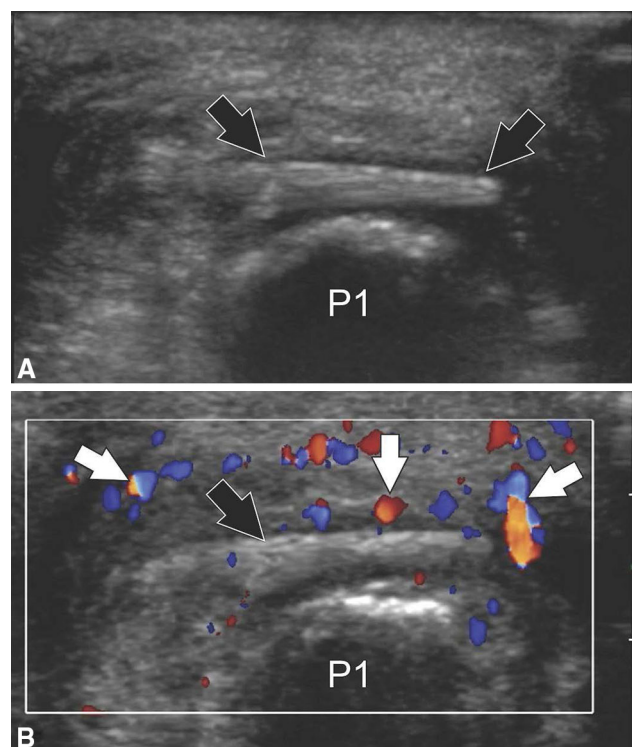
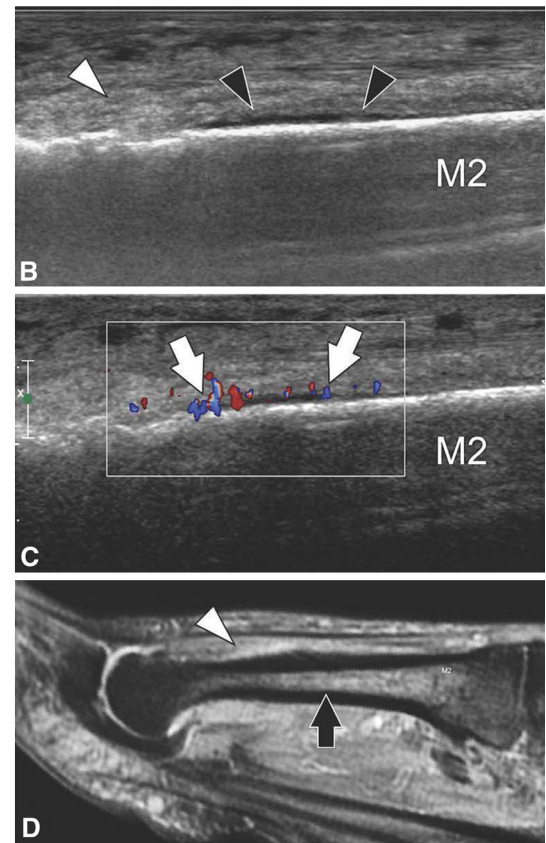
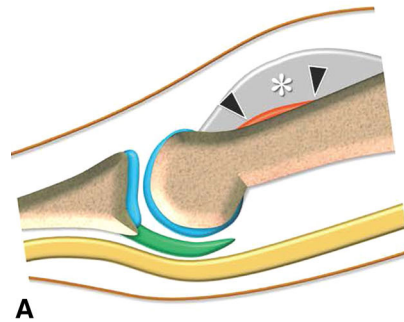


Fig. 18 US appearance of metatarsal stress fracture. Sagittal drawing (a), sagittal (b) and sagittal color Doppler (c) sonogram and sagittal STIR MR image (d) US depicts the stress fracture of the second metatarsal (M2) as focal a hypoechoic thickening of the periosteum (black arrowheads) surrounded by hyperechoic edema of the adjacent tissues. Color Doppler shows hypervascular changes inside the inflamed periosteum (white arrows). MRI confirms the diagnosis by showing hyperintensity of the bone marrow (black arrow) of the metatarsal diaphysis and surrounding soft tissues



[39] (Fig. 18). An increase in the posterior shadowing of the affected metatarsal can be also observed [39]. Oedema and swelling of the soft tissues surrounding the affected metatarsal are depicted as an ill-defined hyperechoic area.

Conflict of interest Stefano Bianchi declare that he has no conflict of interest.

Human and animal studies The study described in this article did not include any procedures involving humans or animals.

References

- Morvan G, Wybier M, Mathieu P, Vuillemin V, Guérini H, Stérin P et al (2010) Foot imaging. *Rev Prat* 60:335–341
- Bianchi S, Martinoli C (2007) *Ultrasound of the musculoskeletal system*. Springer, Heidelberg
- Ansele G, Lee JC, Healy JC (2010) Musculoskeletal sonography of the normal foot. *Skeletal Radiol* 39:225–242. doi:10.1007/s00256-009-0697-7
- Brasseur JL, Morvan G, Godoc B (2005) Dynamic ultrasonography. *J Radiol* 86:1904–1910
- Bianchi S, Martinoli C (2007) Foot. In: Bianchi S, Martinoli C (eds) *Ultrasound of the musculoskeletal system*. Springer, Heidelberg, pp 835–888
- Draghi F, Robotti G, Jacob D, Bianchi S (2010) Interventional musculoskeletal ultrasonography: precautions and contraindications. *J Ultrasound* 13:126–133
- Bianchi S, Zamorani MP (2007) US guided interventional procedures. In: Bianchi S, Martinoli C (eds) *Ultrasound of the musculoskeletal system*. Springer, Heidelberg, pp 891–917
- Wempe MK, Sellon JL, Sayeed YA, Smith J (2012) Feasibility of first metatarsophalangeal joint injections for sesamoid disorders: a cadaveric investigation. *PM R* 4:556–560. doi:10.1016/j.pmrj.2012.01.011
- Guerini H, Ayrat X, Vuillemin V, Morvan G, Thévenin F, Campagna R et al (2012) Ultrasound-guided injection in osteo-articular pathologies: general principles and precautions. *Diagn Interv Imaging* 93(9):674–679. doi:10.1016/j.diii.2012.06.010
- Thomson CE, Beggs I, Martin DJ, McMillan D, Edwards RT, Russell D et al (2013) Methylprednisolone injections for the treatment of Morton neuroma: a patient-blinded randomized trial. *J Bone Joint Surg Am* 95:790–798. doi:10.2106/JBJS.L.01780
- Hughes RJ, Ali K, Jones H, Kendall S, Connell DA (2007) Treatment of Morton's neuroma with alcohol injection under sonographic guidance: follow-up of 101 cases. *AJR Am J Roentgenol* 188:1535–1539
- Fanucci E, Masala S, Fabiano S, Perugia D, Squillaci E, Varucciu V et al (2004) Treatment of intermetatarsal Morton's neuroma with alcohol injection under US guide: 10-month follow-up. *Eur Radiol* 14:514–518
- Sofka CM, Adler RS (2002) Ultrasound-guided interventions in the foot and ankle. *Semin Musculoskelet Radiol* 6:163–168
- Morvan G, Brasseur J, Sans N (2005) Superficial US of superficial bones. *J Radiol* 86:1892–1903
- Torriani M, Kattapuram SV (2003) Technical innovation: dynamic sonography of the forefoot: the sonographic Mulder sign. *AJR Am J Roentgenol* 180:1121–1123
- Gregg J, Silberstein M, Schneider T, Marks P (2006) Sonographic and MRI evaluation of the plantar plate: a prospective study. *Eur Radiol* 16:2661–2669

17. Gregg JM, Schneider T, Marks P (2008) MR imaging and ultrasound of metatarsalgia—the lesser metatarsals. *Radiol Clin N Am* 46:1061–1078. doi:[10.1016/j.rcl.2008.09.004](https://doi.org/10.1016/j.rcl.2008.09.004)
18. Szkudlarek M, Narvestad E, Klarlund M, Court-Payen M, Thomsen HS, Østergaard M (2004) Ultrasonography of the metatarsophalangeal joints in rheumatoid arthritis: comparison with magnetic resonance imaging, conventional radiography, and clinical examination. *Arthritis Rheum* 50:2103–2112
19. Klocke R, Glew D, Cox N, Blake DR (2001) Sonographic erosions of the rheumatoid little toe. *Ann Rheum Dis* 60:896–904
20. Doty JF, Coughlin MJ (2013) Metatarsophalangeal joint instability of the lesser toes. *J Foot Ankle Surg* 19:S1067–S2516. doi:[10.1053/j.jfas.2013.03.005](https://doi.org/10.1053/j.jfas.2013.03.005)
21. Carlson RM, Dux K, Stuck RM (2013) Ultrasound imaging for diagnosis of plantar plate ruptures of the lesser metatarsophalangeal joints: a retrospective case series. *J Foot Ankle Surg* 52:786–788. doi:[10.1053/j.jfas.2013.05.009](https://doi.org/10.1053/j.jfas.2013.05.009)
22. Abreu E, Aubert S, Wavreille G, Gheno R, Canella C, Cotten A (2013) Peripheral tumor and tumor-like neurogenic lesions. *Eur J Radiol* 82:38–50. doi:[10.1016/j.ejrad.2011.04.036](https://doi.org/10.1016/j.ejrad.2011.04.036)
23. Redd RA, Peters VJ, Emery SF, Branch HM, Rifkin MD (1989) Morton neuroma: sonographic evaluation. *Radiology* 171:415–417
24. Quinn TJ, Jacobson JA, Craig JG, van Holsbeeck MT (2000) Sonography of Morton's neuromas. *Am J Roentgenol* 174:1723–1728
25. Sofka CM, Adler RS, Ciavarra GA, Pavlov H (2007) Ultrasound-guided interdigital neuroma injections: short-term clinical outcomes after a single percutaneous injection—preliminary results. *HSS J* 3:44–49
26. Yap LP, McNally E (2012) Patient's assessment of discomfort during ultrasound-guided injection of Morton's neuroma: selecting the optimal approach. *J Clin Ultrasound* 40:330–334. doi:[10.1002/jcu.21926](https://doi.org/10.1002/jcu.21926)
27. Koski JM (1998) Ultrasound detection of plantar bursitis of the forefoot in patients with early rheumatoid arthritis. *J Rheumatol* 25:229–230
28. Bowen CJ, Culliford D, Dewbury K, Sampson M, Burridge J, Hooper L et al (2010) The clinical importance of ultrasound detectable forefoot bursae in rheumatoid arthritis. *Rheumatology (Oxford)* 49:191–192. doi:[10.1093/rheumatology/kep307](https://doi.org/10.1093/rheumatology/kep307)
29. Bancroft LW, Peterson JJ, Kransdorf MJ (2008) Imaging of soft tissue lesions of the foot and ankle. *Radiol Clin N Am* 46:1093–1103, vii. doi:[10.1016/j.rcl.2008.08.007](https://doi.org/10.1016/j.rcl.2008.08.007)
30. Masih S, Antebi A (2003) Imaging of pigmented villonodular synovitis. *Semin Musculoskelet Radiol* 7:205–216
31. Wan JM, Magarelli N, Peh WC, Guglielmi G, Shek TW (2010) Imaging of giant cell tumour of the tendon sheath. *Radiol Med* 115:141–151. doi:[10.1007/s11547-010-0515-2](https://doi.org/10.1007/s11547-010-0515-2)
32. Potter GK, Feldman JS (1990) Neoplasms of the peripheral nervous system. *Clin Podiatr Med Surg* 7:141–149
33. Bianchi S (2008) Ultrasound of the peripheral nerves. *Joint Bone Spine* 75:643–649. doi:[10.1016/j.jbspin.2008.07.002](https://doi.org/10.1016/j.jbspin.2008.07.002)
34. Bos GD, Esther RJ, Woll TS (2002) Foot tumors: diagnosis and treatment. *J Am Acad Orthop Surg* 10:259–270
35. Boyse TD, Fessell DP, Jacobson JA, Lin J, van Holsbeeck MT, Hayes CW (2001) US of soft-tissue foreign bodies and associated complications with surgical correlation. *Radiographics* 21:1251–1256
36. Nwawka OK, Kabutey NK, Locke CM, Castro-Aragon I, Kim D (2014) Ultrasound-guided needle localization to aid foreign body removal in pediatric patients. *J Foot Ankle Surg* 53:67–70. doi:[10.1053/j.jfas.2013.09.006](https://doi.org/10.1053/j.jfas.2013.09.006)
37. Soubrier M, Dubost JJ, Boisgard S, Sauvezie B, Gaillard P, Michel JL et al (2003) Insufficiency fracture. A survey of 60 cases and review of the literature. *Joint Bone Spine* 70:209–218
38. Bodner G, Stöckl B, Fierlinger A, Schocke M, Bernathova M (2005) Sonographic findings in stress fractures of the lower limb: preliminary findings. *Eur Radiol* 15:356–359
39. Banal F, Etchepare F, Rouhier B, Rosenberg C, Foltz V, Rozenberg S et al (2006) Ultrasound ability in early diagnosis of stress fracture of metatarsal bone. *Ann Rheum Dis* 65:977–978